Multiplanar continuous fiber reinforcement in additively manufactured parts via co-part assembly

Peter G. Kelly, Benjamin H. Gallup and Joseph D. Roy-Mayhew
Markforged, Inc., Waltham, Massachusetts, USA

Abstract

Purpose – Many additively manufactured parts suffer from reduced interlayer strength. This anisotropy is necessarily tied to the orientation during manufacture. When individual features on a part have conflicting optimal orientations, the part is unavoidably compromised. This paper aims to demonstrate a strategy in which conflicting features can be functionally separated into "co-parts" which are individually aligned in an optimal orientation, selectively reinforced with continuous fiber, printed simultaneously and, finally, assembled into a composite part with substantially improved performance.

Design/methodology/approach – Several candidate parts were selected for co-part decomposition. They were printed as standard fused filament fabrication plastic parts, parts reinforced with continuous fiber in one plane and co-part assemblies both with and without continuous fiber reinforcement (CFR). All parts were loaded until failure. Additionally, parts representative of common suboptimally oriented features ("unit tests") were similarly printed and tested.

Findings – CFR delivered substantial improvement over unreinforced plastic-only parts in both standard parts and co-part assemblies, as expected. Reinforced parts held up to 2.5x the ultimate load of equivalent plastic-only parts. The co-part strategy delivered even greater improvement, particularly when also reinforced with continuous fiber. Plastic-only co-part assemblies held up to 3.2x the ultimate load of equivalent plastic only parts. Continuous fiber reinforced co-part assemblies held up to 6.4x the ultimate load of equivalent plastic-only parts. Additionally, the thought process behind general co-part design is explored and a vision of simulation-driven automated co-part implementation is discussed.

Originality/value – This technique is a novel way to overcome one of the most common challenges preventing the functional use of additively manufactured parts. It delivers compelling performance with continuous carbon fiber reinforcement in 3D printed parts. Further study could extend the technique to any anisotropic manufacturing method, additive or otherwise.

Keywords Fused filament fabrication, 3D printing, Continuous carbon fiber reinforcement, Mechanical properties, Anisotropy, Interlayer strength

Paper type Research paper

1. Introduction

Additive manufacturing offers a broad range of advantages over traditional manufacturing processes such as machining and injection molding. Foremost among these advantages are rapid part delivery and design flexibility. A common tradeoff for these advantages is anisotropic material properties – particularly in fused filament fabrication (FFF) 3D printing. The tradeoff is most often realized as reduced strength between manufactured layers (Ma *et al.*, 2021; Zohdi and Yang, 2021; Ahn *et al.*, 2002; Gordelier *et al.*, 2019; Goh *et al.*, 2020; Gao *et al.*, 2021). While proper selection of build orientation can mitigate some impact of this anisotropy (Ćwikła *et al.*, 2017), a single part will frequently have multiple distinct features with conflicting optimal orientations. Additive manufacture of such a part in a single build orientation necessarily produces a compromised final part.

Composite materials are commonly used to improve the material properties of additively manufactured parts (Goh *et al.*, 2018). This reinforcement includes both discontinuous fillers (e.g. chopped glass fiber, carbon black, milled carbon fiber) and continuous reinforcement (e.g. continuous carbon fiber, para-aramid fiber and

The current issue and full text archive of this journal is available on Emerald Insight at: **https://www.emerald.com/insight/1355-2546.htm**

Rapid Prototyping Journal
29/11 (2023) 64–73
Emerald Publishing Limited [ISSN 1355-2546]
[DOI 10.1108/RPJ-12-2022-0415]

The authors would like to acknowledge Jessica Faust and Michael Imburgia for their insights and feedback on the study and Thomas Muscolo for inspiring customer-relevant test part. The authors would like to thank Nicholas Sondej and Alex Crease for the technical content of their reinforcement-themed marketing materials.

Conflict of interest statement: The authors declare conflict of interest as all authors are employees of Markforged.

Source line: All figures and tables are the work of the authors and permission is granted to use them.

Received 15 December 2022
Revised 22 February 2023
13 March 2023
Accepted 16 March 2023

glass fiber). Markforged brand printers in particular can print with both a discontinuously reinforced base material and a variety of continuous reinforcement fibers, including carbon fiber. The continuous reinforcement is a significant improvement, as typical engineering plastics (for example, nylon) will have tensile yield strength near 40 MPa in the printed plane where the inlaid continuous carbon fiber will have up to 800 MPa yield strength – nearly a 20-fold improvement [1]. However, the composite strength is limited to the XY plane in which the fiber is laid. Consequently, the parts are limited to the strength of their parent plastic in the Z direction – a strength already reduced by the additive manufacturing process. (Tekinalp *et al.*, 2014; Goh *et al.*, 2021; Ma *et al.*, 2019)

In many instances, a part can be designed with reinforcement in the plane of loading, yet this is not always the case. There are many approaches to increasing strength in the Z direction of additively manufactured FFF parts such as annealing (Zhang and Moon, 2021), Z-pinning (Duty *et al.*, 2019) and spiral toolpaths (Avdeev *et al.*, 2019), but all of these technologies are limited to plastic strength (as opposed to continuous fiber composite strength). Interlaminar strength can be increased by placing fiber in all directions instead of in just one plane, but routing continuous fiber on more than one plane requires significantly more complex toolpath planning and multi-axis capable hardware, making the technology only appropriate for the most demanding industries, such as aerospace and defense. Furthermore, in some 3D printed parts, not all load-bearing features can be reinforced with in-plane continuous fiber. This limitation could be due to part geometry, support structures, ideal print orientations or other factors (Hooshmand *et al.*, 2021; Fang *et al.*, 2020). In other cases, some individual features, such as snap-fit clips or small posts that are printed in the Z direction may have such low surface area in the XY plane that they are extremely weak and yield or break easily.

This paper proposes a methodology in which such conflicting features can be functionally separated into "co-parts." Non-ideal features can be separated into two or more co-parts by Boolean subtraction, and the now separate co-parts can be simultaneously printed in their ideal orientations with optimal plastic strength as well as optimal continuous fiber orientation. These co-parts are subsequently assembled, sidestepping any build orientation compromises and delivering improved end-part performance. At least one company (9T Labs) uses a similar strategy, but their process requires a separate molding machine and specific tooling to be manufactured for every part geometry [2]. The co-part strategy has the benefit of working on typical three-axis FFF printers without any hardware modifications.

2. Materials and methods

2.1 Materials and printers

3D printing materials and printers used in this study were supplied by Markforged (Watertown, MA, USA). Two 3D printing materials were used: Onyx™, a nylon-based filament reinforced with chopped carbon fibers; and continuous carbon fiber (Continuous Fiber – Carbon). Test specimens were printed on Markforged's Mark Two desktop 3D printers using the company's Eiger™ Software. Print beds were leveled using the print bed leveling utility.

2.2 Printed samples

All samples were printed using solid infill at 125 μm layer height. Parts printed with continuous carbon fiber were either printed with just concentric fiber rings or with isotropic fiber and concentric fiber rings depending on the specific part geometric limitations and top performing continuous fiber reinforcement (CFR) orientation. For each part reinforced with continuous fiber, the settings used in Eiger were optimized to maximize the strength of each part (e.g. concentric fiber rings, fiber fill type, etc.). However, fiber was not used in areas where it was not useful to mimic real-world applications where additional weight and material cost is an important concern. For parts with the concentric fiber fill type, the maximum number of concentric fiber rings that fit inside the part was chosen. Details of each part's fiber settings are specified in Table 1. Co-parts were printed in the same build, with each part oriented in the desired direction – two examples of which can be seen in Figure 1. Co-parts were printed with zero gap allowance between the interfacing surfaces and assembled by press fitting them together with an arbor press. Test specimens were dried for 48 h at 75°C

Table 1 Fiber print settings used for generating fiber tool paths in Markforged Eiger software

Part	Category	Fiber layers	Fiber fill type	Concentric fiber rings
Pole Clip	CFR Orientation 1	116–226	Concentric	8
	CFR Orientation 2	50–220	Concentric	8
	Fiber Co-part A	40–151	Concentric	8
	Fiber Co-part B	5–136	Concentric	8
Mounting Plate	CFR Orientation 1	228–288, 364–416	Concentric	4
	CFR Orientation 2	5–16, 33–44	Isotropic	2
	Fiber Co-part A	5–370	Concentric	4
	Fiber Co-part B	5–44	Isotropic	2
Snap-fit clip	Fiber Co-part A	5–77	Concentric	4
	Fiber Co-part B	5–53	Concentric	4
Post	Fiber Co-part A	5–77	Concentric	4
	Fiber Co-part B	5–53	Concentric	4
Loop	Fiber Co-part A	5–77	Concentric	4
	Fiber Co-part B	5–53	Concentric	4

Figure 1 Build view in Markforged's Eiger software showing print orientations of (a) pole clip and (b) mounting plate co-parts

(a) (b)

under vacuum immediately prior to testing to reduce variability due to environmental factors (Faust *et al.*, 2021).

We printed five types of demonstration parts which represent a variety of use cases. For each type, three parts were printed and tested. Demonstration prints include full parts (i.e. pole clip and mounting plate) and individual features (i.e. snap-fit clip, post and loop). Full part and individual feature load cases are shown in Figure 2 and Section 3.2, respectively. To test full parts, we printed parts in four different print strategies:

1 plastic monoliths;
2 plastic co-parts;
3 plastic with CFR; and
4 plastic with CFR co-parts.

To understand the effect of print direction and ensure that we were not underestimating our plastic or composite part mechanical properties, we printed parts in different orientations and looked for the highest performing parts for each cohort. For individual features, we printed these parts using three different print strategies: plastic monoliths, plastic co-parts, plastic with CFR co-parts. The individual feature test parts were printed in non-ideal orientations for plastic monoliths while the co-parts were printed in ideal orientations. This is because in some real applications where ideal orientation of the overall part may take precedence over some localized geometries, these individual features must be printed in a poor orientation and accept poor mechanical properties or be separated into co-parts.

2.3 Mechanical testing

All mechanical testing was conducted on an Instron 3369 with a 50 kN load cell. Samples were tested such that forces applied best mimicked the desired use cases of the parts. For instance, Figure 2 shows a pole clip being secured through one hole axis and being pulled from the second hole axis.

Figure 2 Load case of (a) pole clip and (b) mounting plate demonstration parts

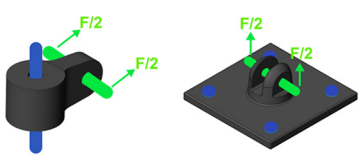

(a) (b)

Custom fixtures were designed to accommodate the test specimens. Figure 3 shows a custom mounting plate providing repeatable support to the snap-fit clip while the test head is lowered. Three samples were tested in each case, with average and standard deviation provided.

3. Results and discussion

The practical application of co-parts is first presented in Section 3.1. In this, two representative parts are analyzed with regards to their mechanical performance when produced with traditional plastic FFF, traditional continuous carbon fiber reinforced FFF, and using co-part assembly. Design factors which affect properties – such as build orientation and CFR pathing – are discussed as are the failure mechanisms. Overall we show that parts with CFR can withstand over 1.5x the load of the control monolithic plastic part before failure, whereas fiber reinforced co-parts can withstand over 3x the load. Section 3.2 then analyzes three unit tests, which explore how individual features – snap-fit clips, posts and loops – can be reinforced. Co-parts of cylindrical posts showed the greatest benefit – withstanding over 6x the maximum load of traditional plastic parts. Finally, Section 3.3 discusses general design guidance for co-parts based on the observed results – most

Figure 3 Snap-fit clip being tested with Instron test fixture

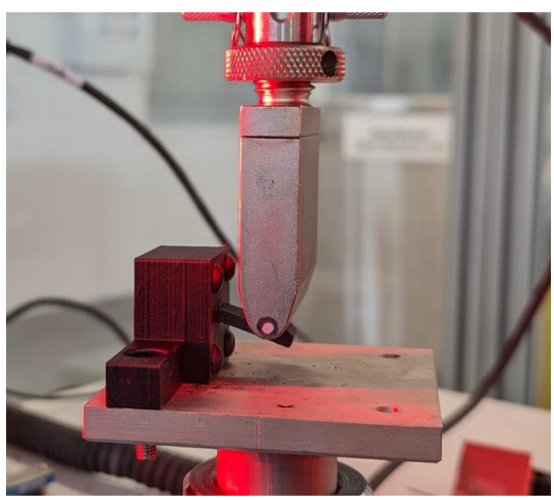

crucially that load transfer between the co-parts must be carefully considered in all cases.

3.1 Full-part reinforcement

To address the broadest set of metal replacement applications, a CFR composite part should be reinforced in multiple planes, corresponding to where load is applied. Entire parts can be reinforced in multiple planes using the co-part assembly method. Figure 4 shows the print orientations of two monolithic parts selected for this study. The first part demonstrated is a pole clip with two holes that are oriented in two different planes offset by 90°. For reference, the load case for this part is shown in Figure 2(a). This scenario is common in many end-use parts and makes reinforcement of both holes impossible with only one plane of reinforcement. Figure 5 shows the co-part separation and reinforcement strategy where the original part is separated into three co-parts which are printed in the same build. This enables fiber to be routed around each hole, reinforcing it more effectively that the base plastic resin can. The dual pathing also prevents the part from failing due to delamination of plastic and fiber layers which can happen when sufficient force is applied perpendicular to the pathing plane.

For a monolithic thermoplastic pole clip being printed in Orientation 1, the maximum load was 2.6 times greater than when printed in Orientation 2 (Figure 6). Herein, the best performing monolithic part is used as our control – Orientation 2 for this part. As would be expected, the control part failed along the geometry with the lowest cross-sectional area, at a load of 8.5 kN. The maximum load sustained by this geometry was significantly increased by the addition of continuous fiber in one plane in the weakest area of the part: the thinner of the two through holes. Similar to the monolithic plastic part, the single plane fiber parts were tested in multiple orientations. When printed in Orientation 1, the part printed with CFR reached 210% the load of the control and failed due to cracks propagating along the fiber and thermoplastic layers [Figure 7(b)]. CFR orientation 2 [Figure 7(c)] performed worse than the plastic-only control sample in Orientation 1 and only 1.3x better than the control sample in Orientation 2. This result can be explained due to the part being printed in an orientation where a region of the part with a much lower cross sectional area is not reinforced with continuous fiber, causing it to fail in shear at a much lower maximum load than in Orientation 1. In this case, the fiber does nothing to increase the strength of the part, as the interlayer adhesion of the thermoplastic fails before the fiber would fail in tension.

Figure 5 (a) Original pole clip part printed as one monolith; (b) assembled co-part made up of three pieces, where end pieces are colored blue, the core is colored red, and fiber traces are in white; (c) assembly strategy for the co-part

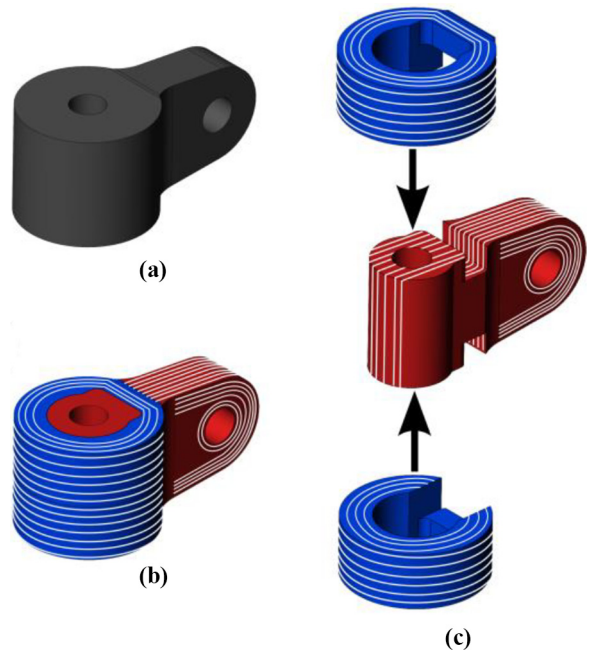

In end-use applications, it is critical to properly select the print orientations of additively manufactured composite parts and fiber pathing, so that they are loaded in directions and regions of highest strength due to their anisotropy. This insight also applies to co-parts. The thermoplastic-only co-part [Figure 7(d)] performed nearly identically to the control (8.7 kN), as it failed in a similar manner. In this case, separating the part into co-parts printed in their preferred orientations had no effect, as the thinner section of the part was already printed in its preferred orientation in the control part. However, when the co-parts are printed with continuous carbon fiber reinforcement [Figure 7(e)] they sustain over 21 kN on average, which is ~250% the average maximum load the part reaches before failure relative to the control, outperforming the best single plane fiber orientation by about

Figure 4 Print orientations, where the XY plane is parallel to the printed layers and coordinate systems are shown for (a) pole clip Orientation 1 (b) pole clip Orientation 2 (c) mounting plate Orientation 1 (d) mounting plate Orientation 2

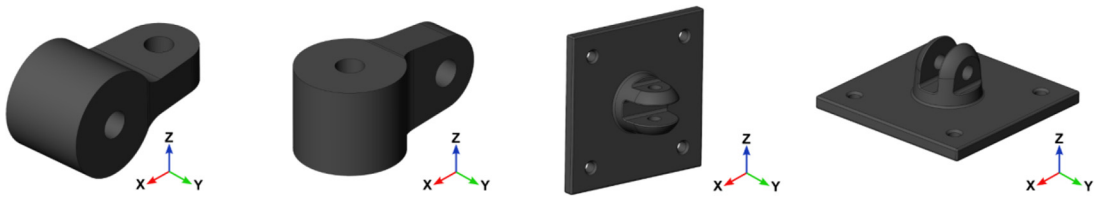

Figure 6 Average maximum load each version of the pole clip reaches prior to failure; plastic only represents our control sample; CFR Orientation 1 and CFR Orientation 2 are shown in Figure 4

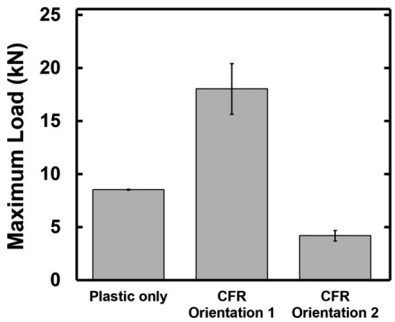

Figure 7 Pole clip demonstration parts after failure, (a) monolithic plastic control, (b) CFR orientation 1, (c) CFR orientation 2, (d) thermoplastic-only co-parts, (e) continuous carbon fiber reinforced co-part

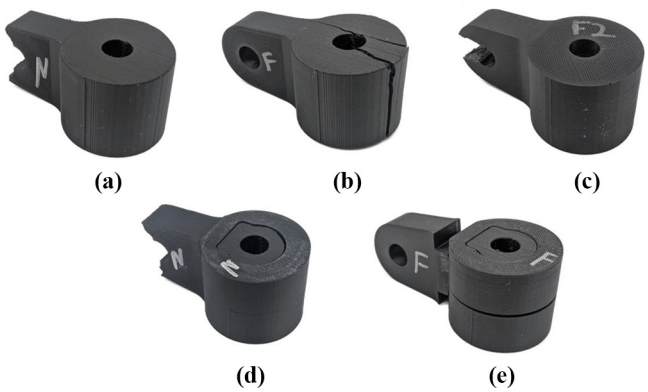

3 kN. The co-part assembly failed due to one co-part component bending and pulling out of the assembly. Further co-part design optimization by adjusting the dimensions of each co-part could result in additional improved performance.

The second part explored was a mounting plate (Figure 8) secured using four bolts and loaded on a centrally located boss with a through hole [for reference, load case is illustrated in Figure 2(b)]. This part is representative of a bracket in a common load case where the direction of load is in a different plane than the surface it is mounted to. When printed as a plastic monolith the control part fails due to layer delamination in the area with the lowest cross-sectional area [Figure 9(b)]. The best-performing fiber orientation is the result of fiber reinforcing the weakest plastic section – the central through holes. Orientation 1 requires significantly more support material than Orientation 2 in addition to a 37% longer print time. In this case [Figure 9(d)], the part failed due to the high stiffness of the fiber in the XY plane and the much lower strength of the interlayer adhesion between continuous fiber and thermoplastic layers. Nevertheless, this part (Orientation 2) showed a 60% improvement in maximum load over the control. This part also had the highest toughness [as represented in the area under the curve in Figure 9(b)] and had a progressive failure. The continuous fiber-reinforced co-parts performed the best, reaching over 300% the sustained maximum load of the control. In this example, the co-part sample failed due to the component with the boss being progressively pulled through the layers of isotropic fill continuous carbon fiber in the plate co-part until failure [Figure 9(d)].

3.2 Unit tests

While sometimes a full part experiences load, as shown in Section 3.1, often specific features of a part are the main candidates for reinforcement. By separating individual features that print in nonoptimal orientations for mechanical strength into co-parts when the overall part drives print orientation, significant improvements in strength can be made. Three features (a snap-fit clip, a cylindrical post, and a loop) were chosen as unit tests (Figure 10) to demonstrate the efficacy of co-part assembly on single features that otherwise may be mechanically weak when 3D printed in certain orientations with FFF. These parts were printed with three different strategies: controls printed as a plastic-only monolithic part; co-parts in their max load sustaining orientations without fiber; and co-parts in their maximum load sustaining orientations with continuous fiber. We allow ourselves to assume that the monolithic plastic-only control parts are forced into poor

Figure 8 (a) Monolithic plastic mounting plate part (b) assembled co-part (c) assembly strategy

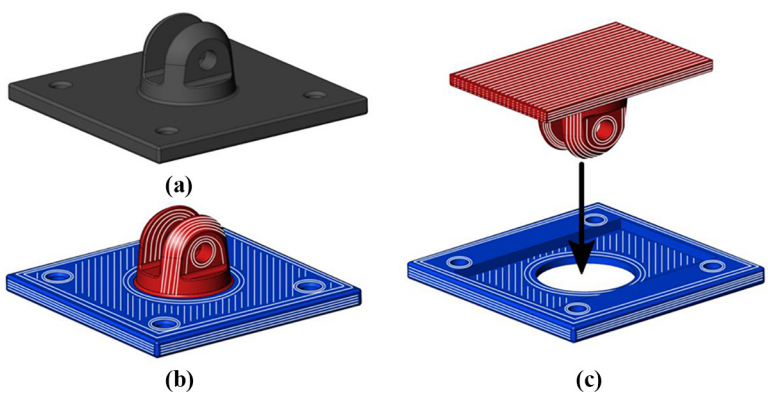

Figure 9 (a) Load vs extension curves for the control, single plane fiber and continuous carbon fiber reinforced co-parts, photographs of (b) monolithic plastic mounting plate after failure, which delaminated between layers in areas of low cross-sectional area, (c) CFR Orientation 1 mounting plate after failure, which cracked in two locations along layer lines, (d) continuous carbon fiber reinforced co-part mounting plate after failure, where one of the co-parts pulled through the other

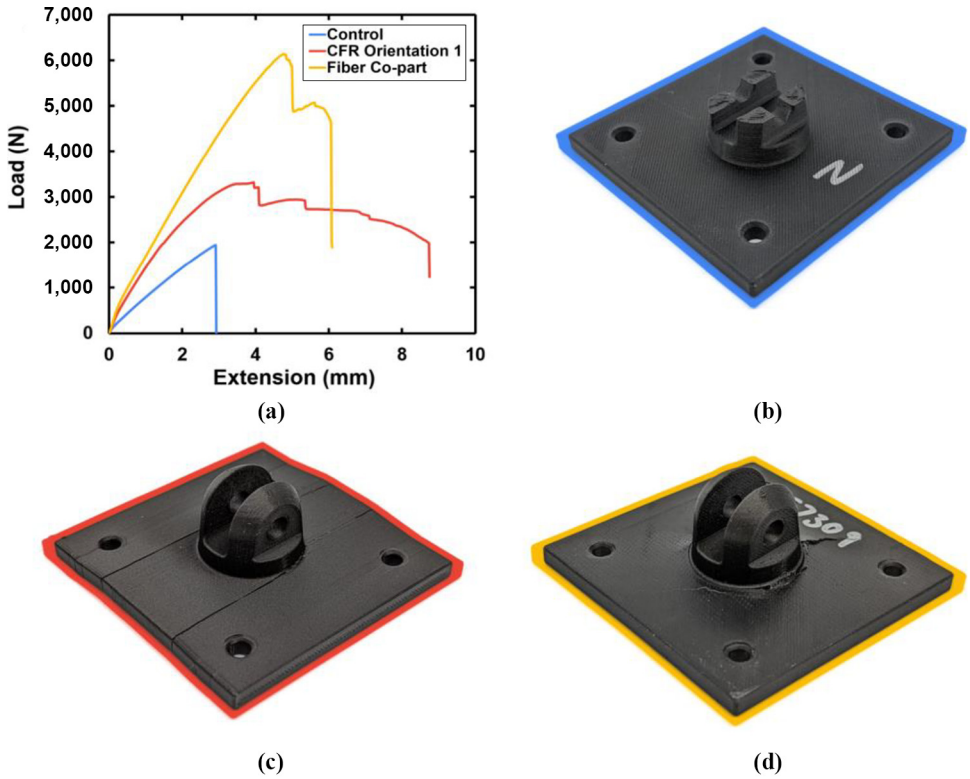

Note: Photographs are highlighted in color for easy reference with (a)

Figure 10 (a) Snap-fit clip, (b) post and (c) loop unit test co-part assembly and load cases

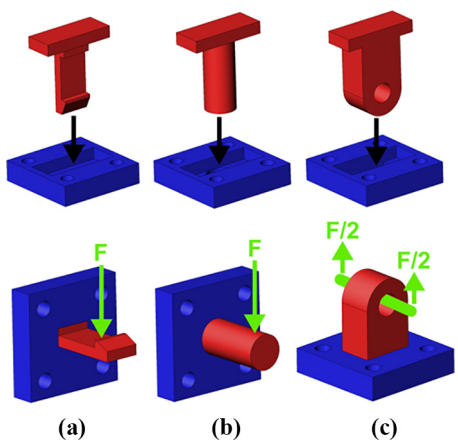

orientations due to the theoretical overall part needing to print in a certain orientation. For the snap fit clip and the posts, load was applied downward 15 mm away from their supported ends, whereas for the loop part, load was applied upward through a pin that goes through the hole.

In each case, as shown in Figure 11, thermoplastic-only co-parts outperformed the control while the continuous fiber reinforced co-parts outperformed both other categories. This result is due to the higher bending strength of the material printed in the XY plane for both printed thermoplastic and continuous fiber materials in comparison to their interlaminar strength. For the snap-fit clip, the plastic-only co-parts and continuous fiber-reinforced co-parts withstood 170% and 410%, respectively, of the maximum load of the monolithic plastic control. An even greater improvement was seen with the post sample. Plastic-only co-parts, and continuous fiber co-parts withstood 320% and 640%, respectively, of the maximum load of the monolithic plastic control. Both the snap-fit clip and post monolithic parts failed due to layer delamination at their bases, whereas the co-parts failed along their fiber and thermoplastic paths in tension.

3.3 Co-part design considerations

Optimal co-part reinforcement requires deliberate consideration. As discussed above, in additive manufacturing processes build orientation must be carefully selected to manage anisotropic performance of the printed part against functional part requirements. The use of composite materials – specifically CFR – can partially mitigate the inherent limitations of FFF parts as demonstrated in Sections 3.1 and 3.2 and noted by Parandoush and Lin (2017). Co-part decomposition can be considered the next step

Figure 11 Average maximum load for control plastic parts, plastic-only co-parts and fiber co-parts for the clip, post and loop unit tests

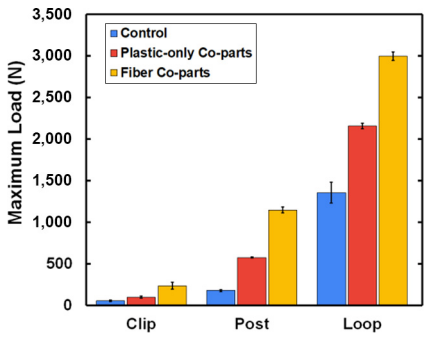

beyond using composite base and reinforcement materials. In effect, they can be considered as a composite of composite parts.

3.3.1 Identifying candidate features

Co-part implementation begins with the identification of competing optimizations of multiple features on one part. Such conflicting optimizations can occur for geometric and/or load-bearing reasons. Example geometric candidates for co-part decomposition include parts with multiple thin protrusions that do not line in a common plane, mounting brackets joining three or more non-coplanar components and many cost, weight or volume-optimized parts. A specific geometric consideration arises around cylindrical features. Critical cylindrical features will have the best mechanical properties and dimensional accuracy when oriented upright – with their axis of revolution perpendicular each manufactured layer. This is due to both the aforementioned reduced Z strength, as well as the quantization of continuous features when sliced into discrete layers. Each layer of an upright circular cross-section is a continuous feature, round to the limits of machine precision, where, conversely, a horizontal circular feature spanning multiple layers is discretized in the slicing process. Now, consider a part with two perpendicular cylindrical features. Individually, each cylinder would both perform best when printed as a stack of concentric, in-plane circles. Due to their perpendicular relative orientation, it is not possible via typical FFF manufacture to print both cylinders in this optimal orientation. Where this simultaneous preferred orientation is not possible, co-parts should be considered, as shown with both the pole clip and mounting plate parts in Section 3.1. Another geometric consideration is aspect ratio. Any high aspect ratio (> 5:1) part not lying in the printed plane is at risk for being snapped off [3]. The height of the high aspect ratio features makes any tip load – expected or otherwise – apply a proportionally large stress at the root of the narrow feature. Compounding the problem, this torque can result in stresses oriented in the lowest-strength direction: across printed layers. The unit testing in Section 3.2 shows that co-parts are particularly effective in this case.

In addition to geometric considerations of a part, load bearing applications for co-part decomposition include essentially any part with loading not parallel to the build platform. For many generatively designed parts, a co-part strategy can be an attractive way to compartmentalize the risks associated with aggressive optimization.

3.3.2 Process overview

If any such competing optimization is identified, the part in question is a prime candidate for co-part implementation. To do so successfully, three principles should be simultaneously considered before the part geometry is finalized for printing:

- separation of features by optimal orientation;
- load transfer between components; and
- assembly

We discuss each in turn.

3.3.2.1 Separation by optimal orientation. This step is generally the simplest of co-part implementation. Optimal orientation of an FFF part is a well-studied problem, both experimentally (Górski, 2015) and procedurally (Hooshmand *et al.*, 2021). Generally speaking, the optimal orientation is one where the principal loads through critical features are carried parallel to the printed layers – minimizing loading in the weakest interlayer direction. However, orientation must also be traded off with print time, support material usage and other factors [4]. Furthermore, when the parts laid flat so loads are in-plane they are ideal candidates for CFR – this is perhaps the most powerful opportunity presented by co-part decomposition. Critical features with low cross-sectional area in the XY plane should be avoided, and co-part print orientation should be selected to avoid this scenario when possible. If this is unavoidable, these features could be decomposed into additional co-parts. This process is depicted in a flowchart in Figure 12. A continuous-fiber capable 3D, Cartesian-style FFF printer – such as the Markforged Mark Two, X7, or FX20 – lays the fibers in the printed plane. The authors found that targeting the optimal orientation to add fiber was usually the driving factor of orientation selection, and not just a beneficial coincidence.

3.3.2.2 Load transfer between components. With the orientation optimized for individual critical feature performance, load transfer between the now-separate co-parts should be considered. While the specifics of doing so are intimately tied to the given unique part geometry, three general strategies are likely useful.

The first and most broadly applicable strategy is to arrange the co-parts such that applied load attempts to pull one part through the other. This strategy is used in the mounting plate and unit tests studied in this study. A flared base to the smaller co-part paired with plate-like reinforcement of the pocket in the mating co-part creates a solid, load-bearing foundation. Note that this type of co-part may be significantly weaker in compression than in tension. While the flare may aid in bearing load under tension, the co-part may bear little to no load in compression. Inserting the co-part sideways into a pocket with both roof and floor can create an assembly that bears both tensile and compressive loads. If the part needs to bear load in all directions, without a secondary means of retention (e.g. bolts, pins or adhesives), there will still be little ability to resist loads back along the insertion direction.

A second strategy is to wrap vulnerable geometries with a custom-shaped ring of reinforcement. A closed ring of continuous fiber can greatly improve a part's ability to bear load.

Finally, a third strategy is to leverage woodworking-style joinery, chiefly dovetails to provide strong connections with the ability to resist multiaxial loads and torques (Fang and Mueller, 2018;

Figure 12 Conceptual flowchart depicting the co-part decomposition process; critical features are elements of a part that are expected to experience relatively high loads

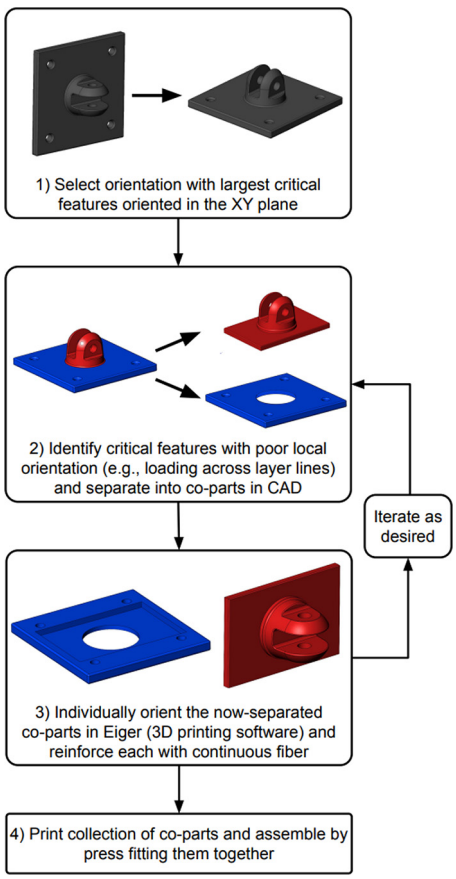

Roche *et al.*, 2015; Emre Ilgın *et al.*, 2022). The broadly studied lessons learned in wood joinery apply well to FFF – particularly with the ability to control continuous fiber placement [5].

3.3.2.3 Assembly. The final assembly of the co-parts may drive the specific geometry required and should be considered before committing to final part design. Broadly speaking, co-parts will either be press- or slip-fit, 2) adhered or 3) bolted or pinned.

For press- or slip-fit applications, some unit-testing may be required to tune the fit. The parts for this study – printed in Onyx on a Markforged Mark Two – had no gap allowance. Zero-gap printing may not work on other printers, in other materials, or for other geometries. Adhesives or epoxies could be used to strengthen the co-part interface under load in all directions. If an adhesive is going to be used, the interface geometry can be simplified – consider a lap joint instead of a dovetail. Markforged recommends Henkel LOCTITE 401, 3 M Scotch-Weld DP100 or 3 M Scotch-Weld DP420 for adhering parts printed in Onyx [6]. For other common 3D printing materials, such as polylactic acid (PLA), polyethylene terephthalate glycol-modified (PETG), and acrylonitrile butadiene styrene (ABS), promising candidates include cyanoacrylate adhesives, epoxies, and silicone glues [7]. In all cases, care must be taken to include gaps between parts to follow manufacturer recommendations for adhesive bond line thickness (Davies *et al.*, 2009). Bolting or pinning will not be covered in detail in this paper, but the authors offer a general recommendation to use heat-set inserts or helicoil-style threaded inserts to provide robust mating threads [8]. By adding bolts or screws with metallic threaded inserts perpendicular to the printed layers of a part, load can be taken up by these components instead of the printed plastic material. However, care must be taken to adequately preload the bolts without driving the parts to compressive failure.

3.3.3 General considerations

Practical implementation of co-part decomposition is generally a straightforward process in the design phase. The parent part can be first designed without consideration for co-parts. Following this, the designer can create blocky geometry with only the co-part mating interface detailed. This can subsequently be used for Boolean subtraction/intersection operations. Tolerances for press-/slip-fit control or adhesive bond line allowance can then be applied.

Running unit tests – small sub-prints where just the co-part interface is isolated – is strongly recommended. A well-designed unit test can have multiple instances of a critical feature with slight variation – effectively isolating the correct critical value in one print. Doing so is a time and resource efficient method for tuning your particular hardware. The authors recommend embedding text into the unit test part (e.g. "+0.1 mm") to aid later differentiation.

While not presented herein, the authors investigated additional interlayer reinforcement methods for FFF 3D printed parts. One effective method was the installation of bolts. However, despite bolt installation being a simpler process, co-parts were instead selected for deeper study, as they do not require sourcing external hardware, have substantially greater geometric flexibility than straight bolts and offer the opportunity for CFR. One particularly valuable lesson was learned: any non-integral reinforcement (such as a bolt) with substantially greater stiffness must be pre-tensioned to provide any significant benefit. In the absence of pre-tension, the parent plastic part initially bears the load and is stretched until failure before the much stiffer reinforcement bears any appreciable load (Oberg *et al.*, 2012). Alternatively, if the reinforcement is adhered along its length, it is now effectively integral to the part, and the authors suspect it will more effectively reinforce the part.

4. Conclusion

The co-part assembly approach has demonstrated significant potential to mitigate interlayer anisotropy, a challenge in practical implementation of functional additively manufactured parts. This study shows that improved orientation and CFR can make parts that bear 250% of the failure load of the equivalent monolithic plastic part. For individual features, co-part decomposition with CFR reached 640% of the failure load of the equivalent feature printed in its unoptimized orientation. This study provides insight into how additively manufactured co-part assemblies can improve functional performance and application robustness with a minimum of design modification and no additional hardware. These findings have implications for the design and production of high-performance functional parts in a variety of industries.

While the principal focus of this paper was improving load at failure, the co-part strategy can also be used to resolve conflicting optimizations for any anisotropic property such as dimensional accuracy, stiffness, surface finish, thermal or electrical conductivity, air flow or any other property of interest. Ostensibly, this approach can be extended to not just any anisotropic properties but also any anisotropic fabrication process, additive or otherwise.

Integrating research into optimal orientation of FFF parts with co-parts can make a powerful contribution to high-performance, low-effort co-part design. Relatedly, Markforged has recently launched its slicer-integrated computational simulation service which has an optimization feature. The authors envision a future where such tightly integrated simulation can power the automatic identification of co-part opportunities. The simplest use of such a system would be to flag co-part opportunities for user implementation and suggest common compatible geometries. An advanced version could automatically implement the full strategy – modeling a mating interface, generating separated co-parts, setting appropriate gaps and compositing a single-print build of all associated co-parts – all with minimal user intervention.

Notes

1 Markforged composites material datasheet, REV 5.2 - 1/20/2022, available at: www-objects.markforged.com/craft/materials/CompositesV5.2.pdf (accessed 6 December 2022).

2 9T Labs hardware, available at: www.9tlabs.com/technology/hardware (accessed 15 February 2023).

3 Markforged design guide for 3D printing with composites, version 1.4, available at: https://static.markforged.com/downloads/CompositesDesignGuide.pdf (accessed 8 December 2022).

4 Design for 3D printing part 3: decreasing print time, available at: https://markforged.com/resources/blog/design-for-3d-printing-part-3-decreasing-print-time (accessed 16 February 2023).

5 3D Printed joinery: simplifying assembly, available at: https://markforged.com/resources/blog/joinery-onyx (accessed 8 December 2022).

6 Bonding markforged plastic parts to other materials, available at: https://support.markforged.com/portal/s/article/Bonding-Markforged-Plastic-Parts-to-Other-Materials (accessed 16 February 2023).

7 Gluing 3D prints: The best glue for PLA, ABS & PETG, available at: https://all3dp.com/2/gluing-3d-printed-best-ways-bond-3d-prints/ (accessed 21 February 2023).

8 Using heat set inserts, available at: https://markforged.com/resources/blog/heat-set-inserts (accessed 16 February 2023).

References

Ahn, S., Montero, M., Odell, D., Roundy, S. and Wright, P.K. (2002), "Anisotropic material properties of fused deposition modeling ABS", *Rapid Prototyping Journal*, Vol. 8 No. 4.

Avdeev, A., Shvets, A., Gushchin, I., Torubarov, I., Drobotov, A., Makarov, A., Plotnikov, A., et al. (2019), "Strength increasing additive manufacturing fused filament fabrication technology, based on spiral toolpath material deposition", *Machines*, Vol. 7 No. 3.

Ćwikła, G., Grabowik, C., Kalinowski, K., Paprocka, I. and Ociepka, P. (2017), "The influence of printing parameters on selected mechanical properties of FDM/FFF 3D-printed parts", *IOP Conference Series: Materials Science and Engineering*, Vol. 227.

Davies, P., Sohier, L., Cognard, J.-Y., Bourmaud, A., Choqueuse, D., Rinnert, E. and Créac'hcadec, R. (2009), "Influence of adhesive bond line thickness on joint strength", *International Journal of Adhesion and Adhesives*, Vol. 29 No. 7.

Duty, C., Failla, J., Kim, S., Smith, T., Lindahl, J. and Kunc, V. (2019), "Z-Pinning approach for 3D printing mechanically isotropic materials", *Additive Manufacturing*, Vol. 27.

Emre Ilgın, H., Karjalainen, M. and Koponen, O.-P. (2022), "Review of the current state-of-the-Art of Dovetail massive wood elements", *Engineered Wood Products for Construction*, Books on Demand, Norderstedt.

Fang, D. and Mueller, C. (2018), "Joinery connections in timber frames: analytical and experimental explorations of structural behavior", *Proc Annual IASS Symp 2018*, pp. 1-8.

Fang, G., Zhang, T., Zhong, S., Chen, X., Zhong, Z. and Wang, C.C.L. (2020), "Reinforced FDM: multi-axis filament alignment with controlled anisotropic strength", *ACM Transactions on Graphics*, Vol. 39 No. 6, p. 204.

Faust, J.L., Kelly, P.G., Jones, B.D. and Roy-Mayhew, J.D. (2021), "Effects of coefficient of thermal expansion and moisture absorption on the dimensional accuracy of carbon-reinforced 3D printed parts", *Polymers*, MDPI AG, 21 October.

Gao, X., Qi, S., Kuang, X., Su, Y., Li, J. and Wang, D. (2021), "Fused filament fabrication of polymer materials: a review of interlayer bond", *Additive Manufacturing*, Vol. 37, p. 101658.

Goh, G.D., Toh, W., Yap, Y.L., Ng, T.Y. and Yeong, W.Y. (2021), "Additively manufactured continuous carbon fiber-reinforced thermoplastic for topology optimized unmanned aerial vehicle structures", *Composites Part B: Engineering*, Vol. 216, p. 108840.

Goh, G.D., Yap, Y.L., Agarwala, S. and Yeong, W.Y. (2018), "Recent progress in additive manufacturing of fiber reinforced polymer composite", *Advanced Materials Technologies*, Vol. 4 No. 1, p. 8.

Goh, G.D., Yap, Y.L., Tan, H.K.J., Sing, S.L., Goh, G.L. and Yeong, W.Y. (2020), "Process–structure–properties in polymer additive manufacturing via material extrusion: a review", *Critical Reviews in Solid State and Materials Sciences*, Vol. 45 No. 2, pp. 113-133.

Gordelier, T.J., Thies, P.R., Turner, L. and Johanning, L. (2019), "Optimising the FDM additive manufacturing process to achieve maximum tensile strength: a state-of-the-art review", *Rapid Prototyping Journal*, Vol. 25 No. 6.

Górski, F., Wichniarek, R., Kuczko, W. and Andrzejewski, J. (2015), "Experimental determination of critical orientation of ABS parts manufactured using fused deposition modelling technology", *Journal of Machine Engineering*, Vol. 15 No. 4, pp. 121-132.

Hooshmand, M.J., Mansour, S. and Dehghanian, A. (2021), "Optimization of build orientation in FFF using response surface methodology and posterior-based method", *Rapid Prototyping Journal*, Vol. 27 No. 5.

Ma, C., Faust, J. and Roy-Mayhew J.D. (2021), "Drivers of mechanical performance variance in 3D -printed fused filament fabrication parts: an Onyx FR case study", *Polymer Composites*, Vol. 42 No. 9, pp. 4786-4794, doi: 10.1002/pc.26187.

Ma, G., Li, Z., Wang, L., Wang, F. and Sanjayan, J. (2019), "Mechanical anisotropy of aligned fiber reinforced composite for extrusion-based 3D printing", *Construction and Building Materials*, Vol. 202, pp. 770-783.

Oberg, E., Jones, F., Horton, H. and Ryffel, H. (2012), "Torque and tension in Fasteners", in McCauley, C. (Ed.), *Machinery's Handbook*, Industrial Press, New York, NY, pp. 1521-1534.

Parandoush, P. and Lin, D. (2017), "A review on additive manufacturing of polymer-fiber composites ", *Composite Structures*, Vol. 182.

Roche, S., Robeller, C., Humbert, L. and Weinand, Y. (2015), "On the semi-rigidity of dovetail joint for the joinery of LVL panels", *European Journal of Wood and Wood Products*, Vol. 73 No. 5.

Tekinalp, H.L., Kunc, V., Velez-Garcia, G.M., Duty, C.E., Love, L.J., Naskar, A.K., . . . and Ozcan, S. (2014), "Highly oriented carbon fiber–polymer composites via additive manufacturing", *Composites Science and Technology*, Vol. 105, pp. 144-150.

Zhang, Y. and Moon, S.K. (2021), "The effect of annealing on additive manufactured ULTEM^{TM} 9085 mechanical properties", *Materials*, Vol. 14 No. 11.

Zohdi, N. and Yang, R.C. (2021), "Material anisotropy in additively manufactured polymers and polymer composites: a review", *Polymers*, Vol. 13 No. 19.

Corresponding author

Joseph D. Roy-Mayhew can be contacted at: joe.roy-mayhew@markforged.com